U.S. DEPARTMENT OF COMMERCE/Environmental Science Services Administration

Technical Report

RESEARCH LABORATORIES

ERL 119-SDL 10

Solar Proton Monitoring System

G. W. ADAMS

L. R. MEGILL

AUGUST 1969

Boulder, Colorado

ESSA RESEARCH LABORATORIES

The mission of the Research Laboratories is to study the oceans, inland waters, the lower and upper atmosphere, the space environment, and the earth, in search of the understanding needed to provide more useful services in improving man's prospects for survival as influenced by the physical environment. Laboratories contributing to these studies are:

Earth Sciences Laboratories: Geomagnetism, seismology, geodesy, and related earth sciences; earthquake processes, internal structure and accurate figure of the Earth, and distribution of the Earth's mass.

Atlantic Oceanographic Laboratories and Pacific Oceanographic Laboratories: Oceanography, with emphasis on ocean basins and borders, and oceanic processes; sea-air interactions; and land-sea interactions. (Miami, Florida)

Atmospheric Physics and Chemistry Laboratory: Cloud physics and precipitation; chemical composition and nucleating substances in the lower atmosphere; and laboratory and field experiments toward developing feasible methods of weather modification.

Air Resources Laboratories: Diffusion, transport, and dissipation of atmospheric contaminants; development of methods for prediction and control of atmospheric pollution. (Silver Spring, Maryland)

Geophysical Fluid Dynamics Laboratory: Dynamics and physics of geophysical fluid systems; development of a theoretical basis, through mathematical modeling and computer simulation, for the behavior and properties of the atmosphere and the oceans. (Princeton, New Jersey)

National Hurricane Research Laboratory: Hurricanes and other tropical weather phenomena by observational, analytical, and theoretical means; hurricane modification experiments to improve understanding of tropical storms and prediction of their movement and severity. (Miami, Florida)

National Severe Storms Laboratory: Tornadoes, squall lines, thunderstorms, and other severe local convective phenomena toward achieving improved methods of forecasting, detecting, and providing advance warnings. (Norman, Oklahoma)

Space Disturbances Laboratory: Nature, behavior, and mechanisms of space disturbances; development and use of techniques for continuous monitoring and early detection and reporting of important disturbances.

Aeronomy Laboratory: Theoretical, laboratory, rocket, and satellite studies of the physical and chemical processes controlling the ionosphere and exosphere of the earth and other planets.

Wave Propagation Laboratory: Development of new methods for remote sensing of the geophysical environment; special emphasis on propagation of sound waves, and electromagnetic waves at millimeter, infrared, and optical frequencies.

Institute for Telecommunication Sciences: Central federal agency for research and services in propagation of radio waves, radio properties of the earth and its atmosphere, nature of radio noise and interference, information transmission and antennas, and methods for the more effective use of the radio spectrum for telecommunications.

Research Flight Facility: Outfits and operates aircraft specially instrumented for research; and meets needs of ESSA and other groups for environmental measurements for aircraft. (Miami, Florida)

ENVIRONMENTAL SCIENCE SERVICES ADMINISTRATION

BOULDER, COLORADO

U. S. DEPARTMENT OF COMMERCE
Maurice H. Stans, Secretary

ENVIRONMENTAL SCIENCE SERVICES ADMINISTRATION
Robert M. White, Administrator

RESEARCH LABORATORIES
George S. Benton, Director

ESSA TECHNICAL REPORT ERL 119-SDL 10

Solar Proton Monitoring System

G. W. ADAMS

L. R. MEGILL

SPACE DISTURBANCES LABORATORY
BOULDER, COLORADO
August 1969

For sale by the Superintendent of Documents, U.S. Government Printing Office, Washington, D.C. 20402
Price 50 cents

TABLE OF CONTENTS

ABSTRACT

A real-time solar-proton monitoring system with ground-based sensors is located in Alaska and other parts of the United States, Greenland, and Canada. A computer in Anchorage, Alaska, interrogates the sensors, processes the data, and transmits the information via teletype to the Solar Forecast Center in Boulder, Colorado. This report describes the physics of the system, i.e., the characteristics of the events (PCA's, auroras, SID's, REP's, and solar noise bursts), how the sensors (riometers, VLF phase and amplitude, forward scatter, neutron monitors, and magnetometers) respond to these events, how these characteristics are programmed to detect the different events, and how the sensor readings are used to obtain information about solar protons. A second report will give details on a set of rocket experiments to be fired into PCA events.

Key Words: Aurora, computers, event description, forward scatter, neutron monitor, PCA event, radiation, real-time detection, REP, riometer, SID, solar noise burst, VLF.

SOLAR PROTON MONITORING SYSTEM

G. W. Adams and L. R. Megill

1. INTRODUCTION

Recent developments in man's use of the upper atmosphere and space have made it desirable to be able to monitor various types of space disturbances. At the present time, nearly all of the disturbances of current interest involve solar activity. The most disruptive natural event known is the solar proton event, which in its manifestation as observed by radio absorption techniques is known as a polar cap absorption (PCA) event.

The ideal way to observe these phenomena is by satellite-based techniques, and eventually a system for such observations will probably be built. In the meantime, cost and the need for nearly real-time communications from the detection systems have prompted the assembly of a ground-based system that will detect, identify, and monitor various types of geophysical events in terms of the effects of changes in the ionosphere on radio waves.

The philosophy which has been followed is one in which changes in the state of the ionosphere are observed by ground-based techniques,

most of which involve the effects on radio waves. In most cases, new sensors have not been installed for the purpose of building this system. Instead, existing research facilities have been monitored on a noninterference basis. The main efforts have therefore gone into obtaining communication links and into the development of software for event detection in an on-line computer that receives the input data.

For the interpretation of the response of the ionosphere to ionizing radiation, a good deal of information is needed on the effective loss rate of electrons in the atmosphere. Although our understanding is far better than it has been, much remains to be learned if information collected by the ground-based system is to be accurately interpreted. For this reason, a number of rocket shots have been planned, which are designed to be "calibration" shots during PCA s.

This report is divided into two parts. The first volume of the report describes the ground-based system, the definitions used for various geophysical events, criteria for sorting out these events, and, briefly, the use of the data. The authors are well aware that many of the following definitions could be open to controversy; we present them merely as descriptions of what we (and therefore the system) mean by reporting these events, not as unique physical definitions.

A detailed description of the software system used in manipulating the data exists as a working memo. This is meant to be a "repair manual" for the software. The system has two basic parts; one uses the system as a data-handling system, the second uses the data in real time for monitoring and alert systems.

A second report (to be published later) is a description of the rocket package which will be used in the "calibration" portion of this work.

This is a developing project, and this report is therefore primarily a progress report. Much remains to be done, including refinement of the software system in order to make it more versatile, and criteria for identifying various types of events. This latter portion in particular will require considerable study in the future. This report will therefore probably be rapidly outdated but will hopefully serve as an adequate base for future work. The description is largely restricted to what now exists or is so near in the future that we feel reasonably sure that it will exist before this description needs rewriting.

2. THE GROUND-BASED NETWORK

Table 1 lists the sensors currently in the solar proton-monitoring system (SPMS), along with pertinent information.

3. EVENT DESCRIPTIONS

Sudden Ionospheric Disturbance (SID) - This is the general name for all ionospheric disturbances caused by x-rays from solar flares. Since x-rays travel in straight lines, only sunlit portions of the ionosphere are affected. Ionization effects from x-rays normally get larger as the sun gets higher in the sky; this is true for most SID effects.

Table 1. Current Sensors

Channel No.	Station	Sensor	Geographic Location Latitude	Longitude	L Value
04	Wildwood	30 MHz Riometer	60.4°N	151.2°W	3.75
05	Anchorage	30 MHz Riometer	61.2°N	149.85°W	4.2
06	Sheep Mountain	30 MHz Riometer	61.8°N	147.6°W	4.5
07	Paxson	30 MHz Riometer	63.0°N	145.7°W	5.05
08	College	30 MHz Riometer	64.9°N	147.8°W	5.5
09	Ft. Yukon	30 MHz Riometer	66.6°N	145.3°W	6.5
10	Bar 1	30 MHz Riometer	70.0°N	142.5°W	8.0
11	Bar 1	50 MHz Riometer	70.0°N	142.5°W	8.0
12	WWVL-Anchorage	19.9 kHz Amplitude	40.7°N	105.0°W	
13	WWVL-Anchorage	19.9 kHz Phase	(Transmitter)		
14	WWVL-Anchorage	20.0 kHz Amplitude	(Transmitter)		
15	WWVL-Anchorage	20.0 kHz Phase	(Transmitter)		
16	GBR-Anchorage	16.0 kHz Amplitude	52.4°N	1.2°W	
17	GBR-Anchorage	16.0 kHz Phase	(Transmitter)		
18	NAA-Anchorage	17.8 kHz Amplitude	44.6°N	67.3°W	
19	NAA-Anchorage	17.8 kHz Phase	(Transmitter)		
20	Aldra, Norway-Anchorage	12.3 kHz Amplitude	66.4°N	13.2°E	
21	Aldra, Norway-Anchorage	12.3 kHz Phase	(Transmitter)		
22	WWVL-Anchorage	19.9-20.0 kHz Phase Differential			
24	Barrow-Anchorage	23.3 MHz Forward Scatter	71.5°N	156.3°W	
			(Transmitter)		

Table 1. (Continued)

Channel No.	Station	Sensor	Geographic Location Latitude	Longitude	L Value
28	Anchorage	Magnetometer - H component	61.2°N	149.85°W	4.2
29		D component	61.2°N	149.85°W	4.2
30		Z component	61.2°N	149.85°W	4.2
32	WWV-Anchorage	15 MHz Amplitude	40.7°N (Transmitter)	105.0°W	
33	WWV-Anchorage	15 MHz Amplitude - different antenna	(Transmitter)		
34	Adak, Alaska-Anchorage	6 MHz Amplitude	52.0°N	177.0°W	
35	Adak, Alaska-Anchorage	10 MHz Amplitude	(Transmitter)		
53	Thule, Greenland	30 MHz Riometer	76.5°N	68.8°W	>50
55	Thule, Greenland	20 MHz Riometer	76.5°N	68.8°W	>50
56	Thule, Greenland	26 MHz Riometer	76.5°N	68.8°W	>50
57	NPM-Thule	23.4 kHz Phase	21.4°N	158.1°W	
58	NPM-Thule	23.4 kHz Amplitude	(Transmitter)		
59	Jim Creek, Washington-Thule	18.6 kHz Phase	48°N	123°W	
60	Jim Creek-Thule	18.6 kHz Amplitude	(Transmitter)		
61	Thule	50 MHz Riometer	76.5°N	68.8°W	>50
62	Thule	40 MHz Riometer	76.5°N	68.8°W	>50

A sensor at which the sun is 1° above the horizon may not see any SID effect, while a similar sensor with the sun 20° above the horizon may be strongly affected.

Auroral Absorption - Auroral absorption can be defined as radio-wave absorption caused by the release of nonrelativistic trapped particles from the earth's magnetic field into the earth's atmosphere.

Auroral absorption occurs in a wide ring roughly centered around a point (the magnetic pole) close to Resolute Bay, Canada. The center of the zone passes through the middle of Alaska, so most of the auroral-sensitive sensors in Alaska (mainly riometers, nighttime forward scatter circuits, and magnetometers) will be affected some fraction of the time.

The energies of the dumped particles are such that the ionization is at considerably higher altitudes than the PCA ionization. The day-to-night variation in the chemistry of the lower ionosphere causes many changes in the appearance of the different phenomena. However, since these changes occur mainly below 80 km, day-night variations are evidence of low-altitude ionization. As a result, there are often only minor differences between daytime and nighttime auroral absorption.

Relativistic Electron Precipitation Events (REP's) - An REP is basically an auroral absorption caused by high-energy electrons, apparently occurring only during daytime. These events have been studied only briefly, and little detail is known. Tentatively they may be described as having less structure and a larger day-night ratio than normal auroral absorption, and they are therefore more difficult to

distinquish from PCA's. They also affect daytime forward scatter circuits, which also makes REP's difficult to distinguish from PCA's. REP's are still confined to the auroral zone, however, although less localized than most auroras.

Polar Cap Absorption Events (PCA's) - PCA's are caused by solar cosmic rays (primarily protons and α particles) impinging on the earth's atmosphere. The particles enter around the poles because they are guided there by the earth's magnetic field. The particles begin to arrive from 20 min to several hours after a visible flare (for those events which can be associated with a visible flare). Except at very low energies ($\lesssim$ 10 MeV), structure with a time constant of less than several minutes is rarely present. Since many of the particles have energies sufficient to penetrate to altitudes below 75 km, daylight and darkness have markedly different effects on the ionization.

4. SENSOR RESPONSES

4.1 Riometers

Riometers in the 5-100 MHz region measure the signal strength of cosmic radio noise passing through the earth's ionosphere. The signal strength at any time, S_T, is referred to the average, or quiet time, signal strength, S_Q. The absorption of the signal is measured in decibels (dB), where $A(dB) = -10 \log_{10} (S_T/S_Q)$. A decrease in signal strength is therefore given as a positive number, and a decrease by a factor of 2 from the average is an absorption of +3 dB. Unless there is actually radio interference present (either man-made or natural), there can only

be signal decreases (positive absorption).

Because the riometer measures a property of the lower ionosphere, and because part of the lower ionosphere changes drastically from day-to-night, a riometer in daylight can have a response quite different from that of a riometer at night. The responses are as follows:

Sudden Cosmic Noise Absorption (SCNA) - An SCNA, the SID as seen by a riometer, can be as high as several dB, and is characterized by a rapid onset, a slow decay, and a duration of several minutes to an hour. Since the SCNA is caused by solar x-rays, the size of the absorption will depend on how high the sun is in the sky, as well as on the x-ray flux. However, if the sun is high enough to be in the antenna pattern of the riometer, then the SCNA will often be masked by the radio noise generated by the flare. Neither the SCNA nor the radio noise will be seen by a riometer at night.

Auroral Absorption - Auroral Absorption is caused by the release of magnetically trapped radiation into the atmosphere. If the riometer is in the auroral zone, then auroral absorption will be common. The magnitude of the absorption is essentially unlimited, often going to 15 dB, which is near the accuracy limit of the riometer. The distinguishing characteristics of auroral absorption are (1) the lack of a sizeable decrease at night (since the ionization is normally too high to be affected by the low-altitude chemistry changes that give the strong day-night effects seen in polar cap absorption); (2) the large amount of structure normally present in the signal strength (auroral absorption has large variations which are as rapid as the time constants

of the equipment and the ionosphere will allow, while PCA's rarely have significant variations on a scale of less than 15 min; (3) the localization of the effect to the auroral zones; and (4) the lack of detailed agreement between two riometers separated by several hundred kilometers or more.

Relativistic Electron Precipitation (REP) - An REP is caused by the release of trapped electrons with energies greater than ~400 KeV into the atmosphere. Since the REP is just a high-energy auroral absorption, most characteristics on the riometer remain unchanged. The major difference is that the REP has less fine structure than auroral absorption and in that respect is difficult to distinguish from a PCA.

Polar Cap Absorption (PCA) - A PCA is caused by the direct entry of solar cosmic ray particles (primarily protons and α particles) into the atmosphere. Its main characteristics are (1) complete coverage of both polar caps, (2) a lack of fine structure, and (3) a marked change from day-to-night. (The ratio of day-to-night absorption for a given part of an event will vary from 3 to 10, with the large values coming at the start of an event. For convenience this ratio is often given as 5.)

The effect of a PCA on a riometer is the most studied and best understood of the phenomena discussed here, partly because it is the easiest to understand. As a result, many details are known about the way a riometer responds to different energies and intensities of particles. In brief, a riometer responds in daytime to protons with energies from 5 to 80 MeV. The absorption varies as the square root of the intensity of the particles and is also a weaker function of their energy spectrum.

At night, it responds to energies from 5 to 25 MeV, with no simple dependence on the intensity. Plots of solar illumination as a function of time of day and day of year are given in the next section for all the riometer stations now in use.

4.2 Neutron Monitors

Neutron monitors measure, indirectly, protons with energies greater than about 200-1000 MeV. The measured quantity is the counting rate which, because of a number of poorly known quantities, is rarely converted to an absolute flux. During quiet times, the counting rate "background" comes from cosmic radiation. The background varies diurnally (plus terms with longer periods), but these variations are small. It also varies exponentially with atmospheric pressure, but this is normally accounted for when the counting rate is given. Counting rates for disturbed times are then given as the difference in count rates as a percentage of the background (e.g., as "a 6 percent increase in counting rate").

Because a charged particle interacts with the earth's magnetic field a given point on the earth can receive protons only from particular directions in space. As a result, a neutron monitor, at any time, is looking in a particular direction or set of directions. These directions are the so-called acceptance cones for the neutron monitors, and they have been calculated for all the existing monitors. With this as background, the responses are as follows:

SID's, Auroral Absorption, and REP's have no effect on a neutron monitor.

PCA - If the PCA has a sufficient flux of high energy protons and if the neutron monitor is looking in the proper direction in space, then there will be a counting rate increase of as much as several hundred percent. The absence of a counting rate increase indicates that high-energy protons are lacking and/or that the look direction is wrong, not the absence of a PCA. The presence of a counting rate increase is probably the best single indicator that a PCA is ocurring.

Forbush Decrease - The sudden commencement as seen by a neutron monitor. The magnetic storm, aurora, etc., which normally accompany a PCA and follow the start of it by 24-48 hours are caused by the arrival of a "cloud" of low energy particles and magnetic fields. This cloud is sufficient to shield the earth from part of the galactic cosmic radiation, resulting in a decrease in the counting rate. This decrease is approximately coincident with the magnetic storm sudden commencement.

4.3 VLF Measurements

The phase and amplitude of very low frequency (10-50 kHz) radio waves are measured primarily as a source of a good frequency standard, since VLF is very stable compared with HF. Nevertheless, there are measureable effects on the signal which give information about the lower ionosphere. The physics of the phase variations is poorly understood, and a quantitative understanding of the amplitude measurements is nonexistent.

Phase changes are normally measured either in degrees or as the corresponding shift in time of the signal. The relationship between

the two is

$$\Delta\phi\ (\mu s) = \frac{10^6 \cdot \Delta\phi\ (\text{deg.})}{360\ f} \quad .$$

For a frequency of 16 kHz (f = 16,000), 1° of phase corresponds to 5.76 μs. The amplitude is measured in dB relative to the quiet-time signal, as in the case of the riometer.

Sudden Phase Anomaly (SPA) - An SPA is the SID as seen by the VLF phase measurement (there is no corresponding term for the amplitude effect). The phase advance can be as high as 200° and is characterized by a time profile similar to a SCNA on a riometer. The amplitude on a long path generally shows an enhancement, although the proper modal interference can result in an amplitude decrease instead.

Aurora - Auroras have only small effects on long-path VLF.

REP - An REP has no effect on daytime VLF phase and amplitude, but a nighttime phase advance with no accompanying amplitude variation is observed.

PCA - A PCA event is accompanied by both a phase advance and an amplitude decrease. The phase will follow the proton flux in some fashion (as yet undetermined) until the amplitude decreases to the point where the signal is no longer usable for phase measurements. At that point the signal is lost, and no further information is obtained from the VLF. However, a long distance polar-cap path can retain a signal throughout a small PCA event - 5 February 1965, for example.

Because the VLF path is long, and because it measures an integrated effect along the path, VLF tends to be unresponsive to phenomena which

are confined geographically. This is the advantage of the technique for PCA identification. A phase advance of more than 30° should be considered significant; a large PCA can drive the phase through several hundred degrees.

The VLF response to PCA events is affected by day-night variations, but to a lesser extent than riometers. Percentage illumination plots for the two important paths currently in use are attached.

4.4 Forward Scatter

In forward scatter, a VHF signal is transmitted into the lower ionosphere, where some fraction of the signal is scattered from nonuniformities in the electron density. The scattered component of the signal is received and the signal strength is measured. Since the scattering region is around 75 km in the daytime, the scattered signal is essentially a low-altitude monitor. Reflected signals from high altitudes, primarily reflected from sporadic E and meteor trails, are also present occasionally.

SID - Daytime forward scatter will not respond to SID's except in rare cases where the x-rays are abnormally energetic, when the signal will show absorption.

Aurora - Forward scatter does not respond to daytime auroras, but often shows a signal enhancement at night.

REP - Forward scatter will respond to a daytime REP if the particles are being dumped near the midpoint of the path. Daytime forward scatter shows absorption, since there is enough ionization created below the

scattering layer to absorb the signal significantly, in spite of the extra ionization being created simultaneously at the scattering level.

PCA - Forward scatter responds to PCA events in much the same way that it does to REP's; the only major difference is that the nighttime enhancement is usually small compared with the REP enhancement. For daytime conditions, connection can be made between the forward scatter and the riometer measurements. With difference in path langth, path geometry, frequency, etc., taken into account, it has been found that the absorption measured on the Goose Bay-Sondre Stromfjord 32.2 MHz forward scatter circuit is eight times the absoprtion that would be measured by a 30 MHz riometer. Similar factors can be determined for other paths and frequencies. Little is known about the nighttime enhancements.

Table 2. Sensor Responses

The table gives a brief summary of the responses of the sensors. It provides a convenient way of surveying the available data to see if sufficient data is available to uniquely identify the type of event. It is not really self-sufficient; riometer absorption coincident with a flare can be labelled as SCNA without further ado, for example, and conflicting data must be considered in the light of other information. Nevertheless, it should serve as a useful guide to the examination of the data.

	SID	Aurora	REP	PCA
Daytime Polar-Cap Riometer (L > 10)	Absorption (SCNA)	No Absorption**	Never Observed	Absorption
Nighttime Polar Cap Riometer	No Absorption	No Absorption**	Never Observed	Absorption/5*
Daytime Auroral-Zone Riometer	Absorption	Absorption	Absorption	Absorption
Nighttime Auroral-Zone Riometer	No Absorption	Absorption	Not Observed	Absorption/5*
Polar-Cap VLF Phase Measurements	Phase Advance (SPA)	No Change	No change in daytime Phase advance at night	Phase Advance
Polar-Cap VLF Amplitude Measurements	Amplitude Increase	No Change	No Change	Amplitude Decrease
Daytime Forward Scatter	No Change (absorption rarely)	No Change	Absorption	Absorption (Enchancement possible on small soft events)
Nighttime Forward Scatter	No Change	Signal Enhancement	Not Observed	Small Signal Enhancement

* Absorption/10 at start of event; absorption/3 near end of event.

** High-latitude absorption events similar in appearance to aurora do occur, but their cause is presently a matter of speculation.

5. SOLAR ILLUMINATION PLOTS

The plots in this section give the pertinent solar illumination information for some of the sensor locations or paths which are affected by day-night variations. For all of these plots the abscissas are the day of the year and the ordinates are in universal time.

Figure 1 and 2 give the contours of the percent of the VLF paths which are illuminated at 60 km, in steps of 25 percent. Seventy-five percent means that 75 percent of the path is in daylight; the rest of the path is in darkness. These plots are predicated on the assumption that later analysis will show a dependance of the VLF response on the fraction of the path illuminated.

Figures 3 to 11 give the illumination conditions for the riometer stations. Because of the effect of sunlight on riometers, the graph tells only if there is daylight, darkness, or twilight above the the riometer. Here daylight is defined to be when the sun is above the horizon, thus illuminating the entire ionosphere. Nighttime is defined by the absence of sunlight below 100 km, and twilight is when the shadow of the earth is somewhere between 0 and 100 km altitude.

6. COMPUTER PROGRAMMING

At present, the programming for the Anchorage computer is changing continuously. It will probably be another year or two before the system becomes even remotely static. As a result, this section must describe both the way the computer is programmed now and the way we think it will be programmed eventually. The problem with this approach is that very little is known about the behavior of most sensors during the initial phases of different types of events, so that much of the programming will undoubtedly change before it is finished.

The general plan for event detection is to have a simple set of criteria for the sensors which would detect a possible event very rapidly, putting the system into "Alert" status. Once the system goes into Alert, 15 min of data will be collected and analyzed with a more complex set of criteria. If the complex criteria are satisfied, then an "Event" will be declared, the type of event and the probability that it is real will be given, and the pertinent information printed out in Boulder. With this sort of scheme, the neutron monitors have to be considered separately, since, for those events with enough high-energy protons to show up on neutron monitors, they may show a counting rate increase well before the other sensors indicate anything. Since the system will put out "Status" messages hourly when there is no activity, there are five types of messages will come out of the system for event detection: Status, Alert, Event, Neutron Monitor Alert,

and Neutron Monitor Event.

That, in brief, is the way the system is planned to operate eventually. At present, the operation is somewhat different from this. The neutron monitors are not yet connected into the system. Arrangements have been made to connect the neutron monitors at Swarthmore, Pennsylvania; Durham, New Hampshire; and Deep River, Ontario, Canada, via the USAF SOFNET teletype system to Boulder, into an SCC-650 computer, and up to Anchorage on the existing teletype line. At present only Deep River is on the SOFNET circuits, and it cannot be used because the U.S. Air Force connections to the computer in Boulder have not been supplied. Also, only the simple set of criteria (the set planned to trigger the Alert messages) has been programmed, so that both Alert and Event detection are operating from the same set of criteria. If the system stays in Alert for 15 min, an Event is declared.

The criteria currently being used by the system consist of a set of flags - four for each sensor (one for each type of event) - whose values are determined by the computer according to which sensor it is, what the current data value is (compared with quiet-day-curve (QDC) value), and what the sunlight conditions are (daylight, twilight, or darkness, for those sensors which are sunlight sensitive).

The flags are set by the computer every minute, summed, and the sum is normalized to a -1 to +1 scale. Any value of this indicator greater than zero will trigger the Alert indicator. Since the largest and smallest values that a particular flag can have are equal and opposite, normalization is accomplished by dividing the sum of the flags by the

largest possible sum for that time.

The details of the flag values are given in the working memo. Only the basic logic will be discussed here.

The riometer flags are trivalued, one value each for the riometer's received signal strength more than an amount δ above the QDC, the signal strength within δ of the QDC, and the signal strength more than δ below the QDC. VLF amplitude and forward scatter flags are also trivalued, while the VLF phase is bivalued - either close to the QDC or not.

In addition to the four types of events, the system also uses the riometers to detect solar noise bursts by looking for simultaneous increases in the signal strength.

The more complex criteria planned for the Event detection, as opposed to Alert, require not only that the riometer reading, for example, be below the QDC, but also that the trend of the data over the past 15 min be toward increasing absorption. Several simultaneity checks are also made: separate flags are assigned to the simultaneity, or lack thereof, between absorption on the Thule riometers and the northern Alaskan riometers; the latitude profile of absorption (riometer absorption vs magnetic latitude) is examined for characteristics of the different kinds of events; the neutron monitors are examined for counting rate increases in the preceding 12 hours; etc. Undoubtedly these criteria will change and more will be added as more is learned about event characteristics.

7. QUANTITATIVE USES OF THE DATA

Ideally, one would like to use the data in real time during PCA events to determine the intensity and energy spectrum of the solar protons, and to construct an accurate extrapolation of the event so that the future time history of the intensity, energy spectrum, and hence the radiation dosage for the event could be determined. At present, none of this appears to be possible; it is possible, however, (Adams and Juday, 1969) to start with daytime riometer absorption as a function of time, calculate the intensity of protons with energies greater than 11 MeV versus time, calculate hard-spectrum and soft-spectrum limits to the proton energy spectrum versus time, and, finally, determine upper and lower limits to the radiation dosage for the events.

For a constant spectrum, the riometer absorption varies approximately as the square root of the proton intensity. A useful parameter (Van Allen et al., 1964) is

$$H(E, p_o) = J(>E)/A^2, \qquad (1)$$

where $J(>E)$ is the integral intensity of protons above energy E, A is the 30 MHz riometer absorption, and p_o is the e-folding magnetic rigidity of an exponential rigidity spectrum given by

$$J(>E) = J_o \exp(-p/p_o). \qquad (2)$$

In (2), J_o is the total intensity of protons, and p is the rigidity of a proton with energy E. For the energies of concern to riometer work,

relativistic effects are negligible, so that energy and rigidity are related simply by

$$p(\mathrm{MV}) = [1876\ E(\mathrm{MeV})]^{\frac{1}{2}} \quad . \tag{3}$$

H as defined in (1) is a function of p_o. What we will show now is that there is an energy (the "least sensitive energy") for which H is essentially independent of p_o. $H(E, p_o)$ can be calculated for various E's and p_o's directly from (1) and (2) and from the results of Adams and Masley 1966 . $H(E, p_o)$ versus p_o is shown for several values of E in figure 12. Examination of these curves shows that $H(11\ \mathrm{MeV}, p_o)$ varies by less than 10 percent over the range $30 \leq p_o \leq 300$ MV, with an average value of 47 protons/cm^2-sec-ster-dB^2, or (assuming 2 π-isotropy in the atmosphere) 295 protons/cm^2-sec-dB^2. Thus we have

$$J(>11\ \mathrm{MeV}) \simeq 295\ A^2 \tag{4}$$

independent of the value of p_o, where J is in protons/cm^2-sec and A is the 30 MHz riometer absorption in dB. It must be pointed out that this relation is valid only for daytime polar-cap riometer readings. The assumption of exponential rigidity spectra is apparently not critical. A test of (4) has been made for several spectra which are severe departures from exponential rigidity spectra. (The details of these spectra are given by Adams and Masley (1965, table 1).) A comparison of the measured values of J(>11 MeV) and the values determined from (4) is shown in table 3, which shows that the maximum error is approximately 6 percent.

The physical (i.e., nonbiological) measure of radiation dose is the

rad, defined as the deposition of 100 ergs per gram of material at the dose point. This can be expressed as

$$1 \text{ MeV/g} = 1.6 \times 10^{-8} \text{ rad} \tag{5}$$

or, in terms of stopping power,

$$D(\text{rads}) = N \frac{dE}{dx} / 1.6 \times 10^{-8}, \tag{6}$$

where D is the dose in rads, N is the number of monoenergetic particles per square centimeter, 1.6×10^{-8} is the conversion factor in MeV/(rad-g), and the stopping power, dE/dx, is in MeV/(g/cm^2). For particles in an energy spectrum given by $d^2N/dEd\,\Omega$ and a nonisotropic solid-angle distribution of shielding and particle flux, (6) becomes

$$D = \int_{\Omega} \int_{E=0} \frac{dE}{dx} \frac{d^2N}{dEd\,\Omega} \, dD \, d\Omega / 1.6 \times 10^{-8}, \tag{7}$$

where the calculation is performed at the dose point. In analogy to the parameter $H(E, p_o)$ relating proton intensities and riometer absorption, the function $K(E, p_o)$ is defined as

$$K(E, p_o) = J(E, p_o)/D \quad . \tag{8}$$

Here again, we want a value of $E(=E_{LS}$, the "least sensitive energy") for which K does not vary with p_o. This value will depend on the shielding thickness for any realistic problem. Just as for the riometer, it is possible to find an E_{LS} for which K is essentially independent of p_o. The least sensitive energies (E_{LS}) and the corresponding values of $K_{LS}(E_{LS})$ have been calculated as a function of thickness for a spherical shield. The results are shown in figure 13. Also shown in this figure

is the cutoff energy for the shield. Notice that the E_{LS} curve follows the cutoff energy curve, since the Bragg peak in the stopping power curve always puts the most damaging energy near the cutoff energy.

For a more complex shielding geometry, one merely sums over the shielding thicknesses in all directions. Alternatively, one can define an equivalent E_{LS} and K_{LS} for a particular shielding geometry. This has been done, for example, for the Apollo Command Module, for both skin and blood-forming organ (BFO) doses. (The BFO dose is for an additional shielding of 5 cm of body tissue.) Figure 14 shows $K_{skin}(E, p_o)$ and $K_{BFO}(E, p_o)$. As can be seen in this figure, $(E_{LS})_{skin} = 50$ MeV and $(E_{LS})_{BFO} = 130$ MeV, while $K_{LS} \simeq 1.75 \times 10^7$ for both cases.

We now have a way to get from riometer measurements to $J(>11$ MeV), a way to determine the least sensitive energy for a particular shielding geometry, and a way to get from $J(>E_{LS})$ to the radiation dosage without having to know the shape of the energy spectrum. If we could determine $J(>E_{LS})$ from $J(>11$ MeV) without knowing the spectrum, the riometer could be used to determine radiation dosage directly. This, of course, is not possible. We can, however, specify reasonable upper and lower limits for $J(>E_{LS})$.

The relation between $J(>11$ MeV) and $J(>E_{LS})$ can be obtained directly from (2) as

$$J(>E_{LS}) = J(>11 \text{ MeV}) \exp\left[\sqrt{1876}\left(\sqrt{11} - \sqrt{E_{LS}}\right) / p_o\right], \quad (9)$$

where p_o varies with time during a PCA event. In the absence of any other information, the variation of p_o with time can be given as follows. A mass plot of p_o versus time after the start of an event is made for

many PCA events. Upper and lower envelopes and a curve through the middle of the distribution are drawn. At any given time, these three curves give a hard spectrum (large p_o) limit, a soft spectrum limit, and a "typical" value. Such a plot is shown in figure 15, along with three curves given by

$$(p_o)_i = C_i \exp(-t/23) + B_i , \qquad (10)$$

where i=1 for the hard limit, i=2 for the "typical" case, i=3 for the soft limit, and t is given in hours. The values of C_i and B_i are:

$C_1 = 280$ $\qquad$ $B_1 = 70$

$C_2 = 200$ $\qquad$ $B_2 = 50$

$C_3 = 130$ $\qquad$ $B_3 = 20$

The relations can now be assembled to calculate radiation doses from an absorption-versus-time plot from a 30 MHz sunlit polar-cap riometer. The results for the Apollo Command Module, for example, are

$$\text{skin Dose (rads)} = 2.06 \times 10^{-2} \int A^2(t) \exp\left[\frac{-145}{C_i \exp(-t/23) + B_i}\right] dt \qquad (11)$$

$$\text{BFO Dose (rads)} = 2.06 \times 10^{-2} \int A^2(t) \exp\left[\frac{-332}{C_i \exp(-t/23) + B_i}\right] dt. \qquad (12)$$

These equations are conveniently handled on computers or desk calculators, or they can be evaluated graphically.

We have shown that (1) 30 MHz polar-cap riometer measurements can be used to determine the integral proton intensity above 11 MeV (H (E, p_o) is reasonably independent of E, so that comparisons of intensity measure-

ments with riometer measurements will show little spectral sensitivity for any value of E in the range 8 to 15 MeV); (2) a spherical shield of any thickness has a least-sensitive energy such that the dose at the center can be determined from the proton intensity without knowing the spectrum; (3) the dose inside any shielding geometry can be determined either by summing the spherical shield results over all directions or by calculating the least-sensitive energy and the corresponding K_{LS} for that particular case; and (4) the variation of p_o with time (and hence the ratio of J(>11 MeV) to J for any other energy) can be described in terms of upper and lower limits to the previous pattern of solar cosmic ray events. The main virtue of these results is that they allow the calculation of several quantities of interest with a minimum of input data.

Table 3. Comparison of J(> 11 MeV) From Satellite Data and J(> 11 MeV) Derived From (4) for Several Spectra Which Are Severe Departures From Exponential Rigidity Spectra.

Date (1961)	Time (UT)		Spectrum Description 0<E<40	40<E<100	E>100 MeV	J(>11 MeV) from data	J(>11 MeV) from (4)
18 July	1300	J_o	220	220	220	80	76
		p_o	235	235	235		
20 July	0100	J_o	1300	27	195	62	60
		p_o	52	180	98		
20 July	0300	J_o	1300	25	148	38	36
		p_o	47	173	100		
21 July	0200	J_o	820	10	98	20	20
		p_o	47	195	95		
21 July	1000	J_o	620	10	22	17	16
		p_o	42	130	100		
21 July	1400	J_o	610	7	15	17	16
		p_o	40	121	100		

8. ACKNOWLEDGMENTS

The authors gratefully acknowledge the contributions of many people to the development and operation of this system. The Space Disturbances Monitoring Station, directed during this work by Dr. H. J. A. Chivers, Mr. William E. Little, and Mr. Steffen Maagoe, was responsible for setting up the system. The Air Force Cambridge Research Laboratories and the H. R. B. Singer Corporation made data available from the Geopole Station at Thule, Greenland. The University of Alaska operates the riometers at Bar l, Ft. Yukon, and College, Alaska. Mr. Don Smart of the Air Force Cambridge Research Laboratories is mainly responsible for the neutron-monitoring system, which in the future will supply data from Deep River, Ontario, Canada; Swarthmore, Pennsylvania; and Durham, New Hampshire.

Financial support for this work has been given by the Environmental Science Services Administration and by the National Aeronautics and Space Administration, Contract No. T-15237 (G). Some of the communications links have been provided by the U. S. Air Force.

9. REFERENCES

Adams, G. W. and R. D. Juday (1969), Riometer measurements, solar proton intensities and radiation dose rates, Planet. Space Sci. (in press).

Adams, G. W. and A. J. Masley (1965), Production rates and electron densities in the lower ionosphere due to solar cosmic rays, J. Atmosph. Terr. Phys. 27, No. 3, 289-298.

Adams, G. W. and A. J. Masley (1966), Theoretical study of cosmic noise absorption due to solar cosmic radiation, Planet. Space Sci. 14, No. 3, 277-290.

Freier, P. S. and W. R. Webber (1963), Exponential rigidity spectrums for solar-flare cosmic rays, J. Geophys. Res. 68, No. 6, 1605-1629.

Van Allen, J. A., W. C. Lin and H. Leinbach (1964), On the relationship between absolute solar cosmic ray intensity and riometer absorption, J. Geophys. Res. 69, No. 21, 4481-4491.

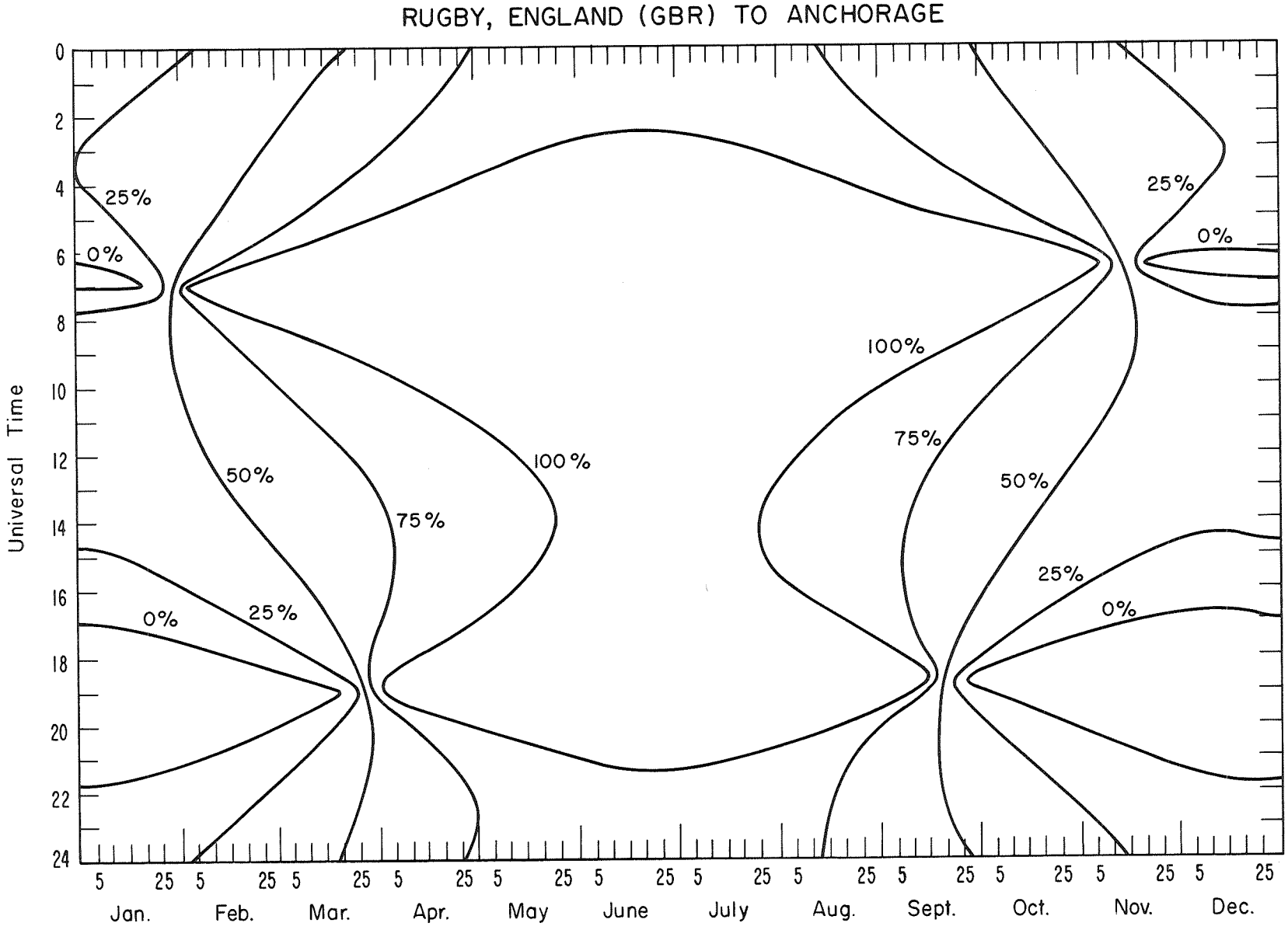

Figure 1. Solar illumination plot - Rugby, England (GBR) to Anchorage.

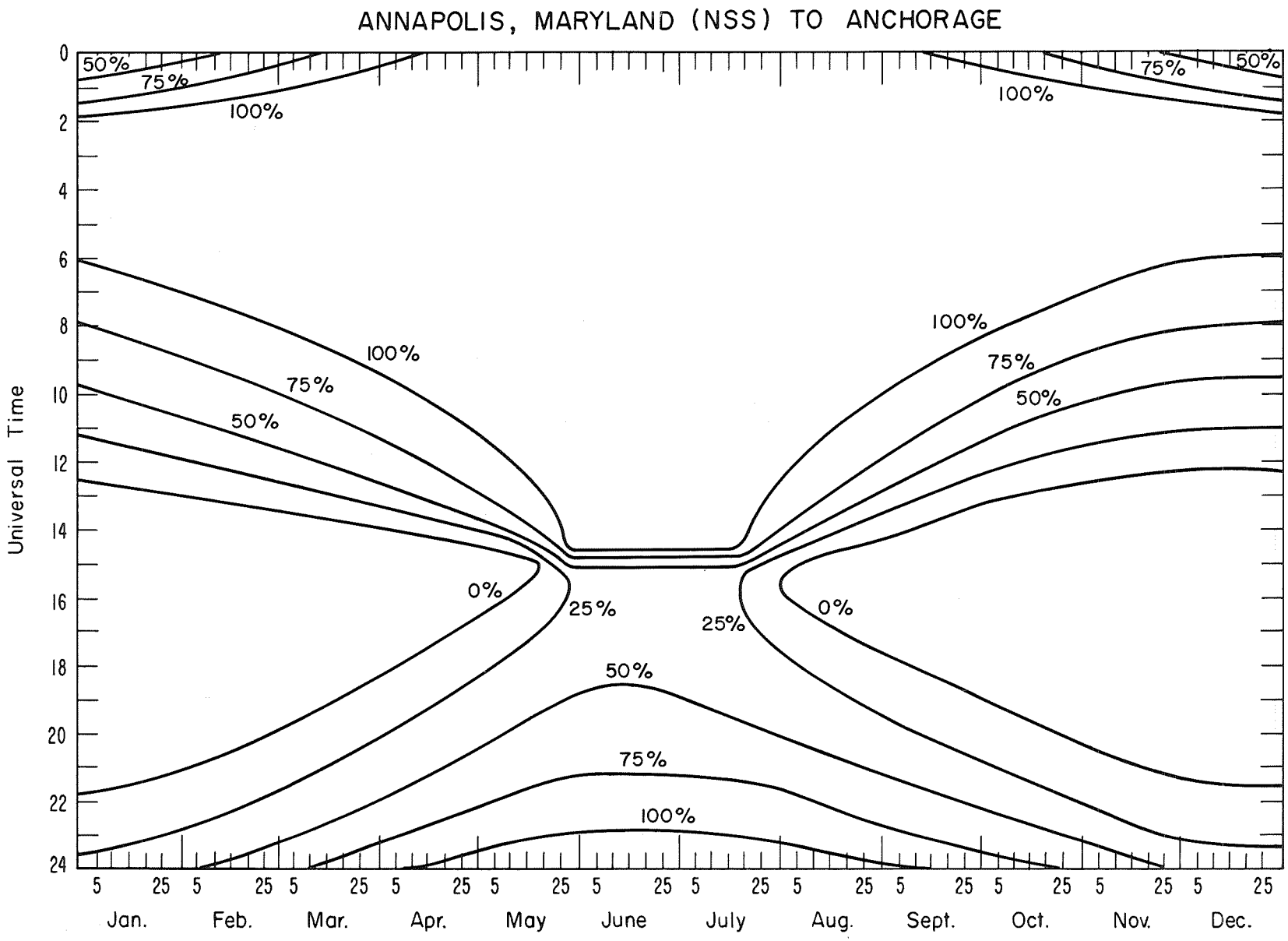

Figure 2. Solar illumination plot - Annapolis, Maryland (NSS) to Anchorage.

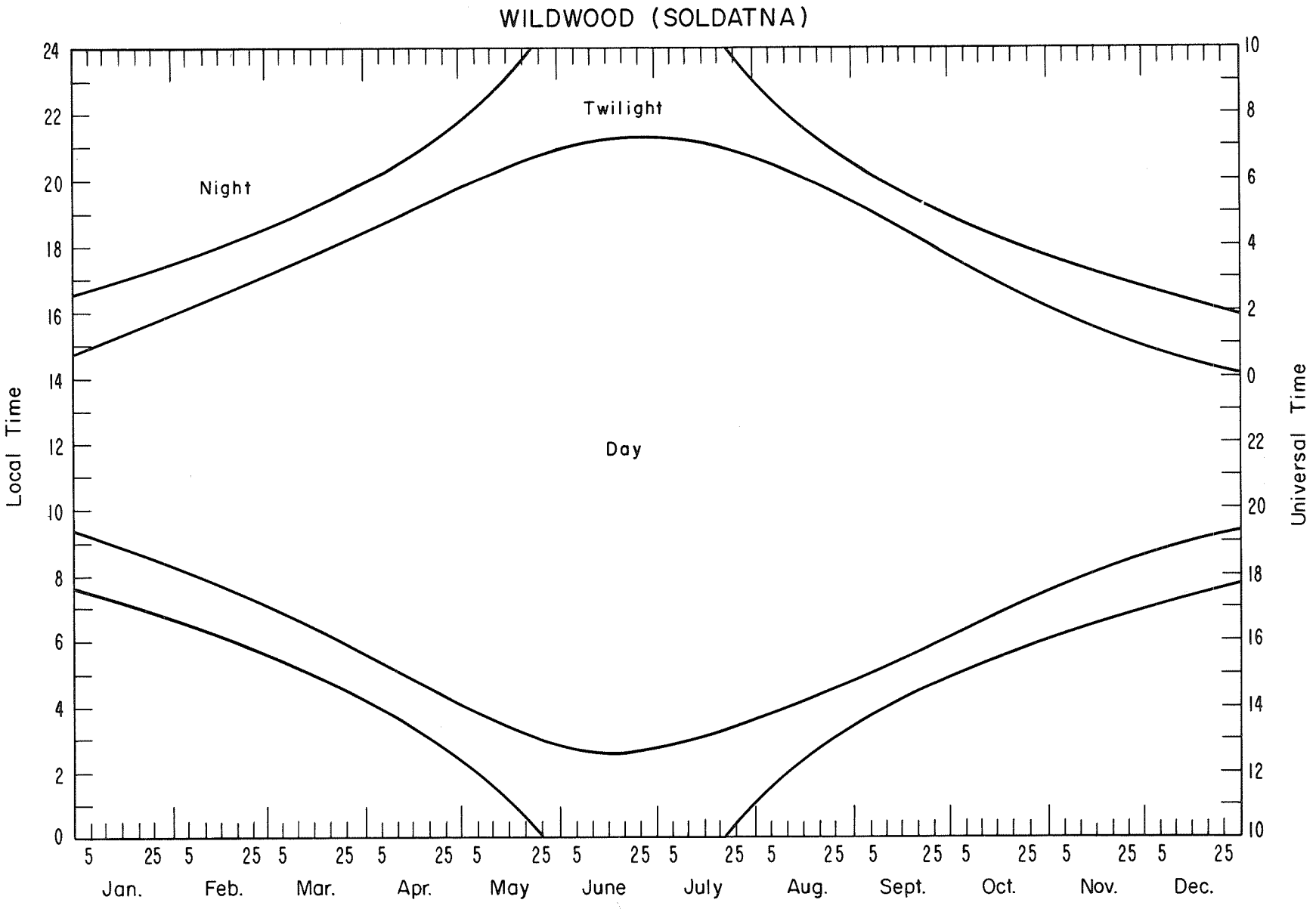

Figure 3. Solar illumination plot - Wildwood (Soldatna).

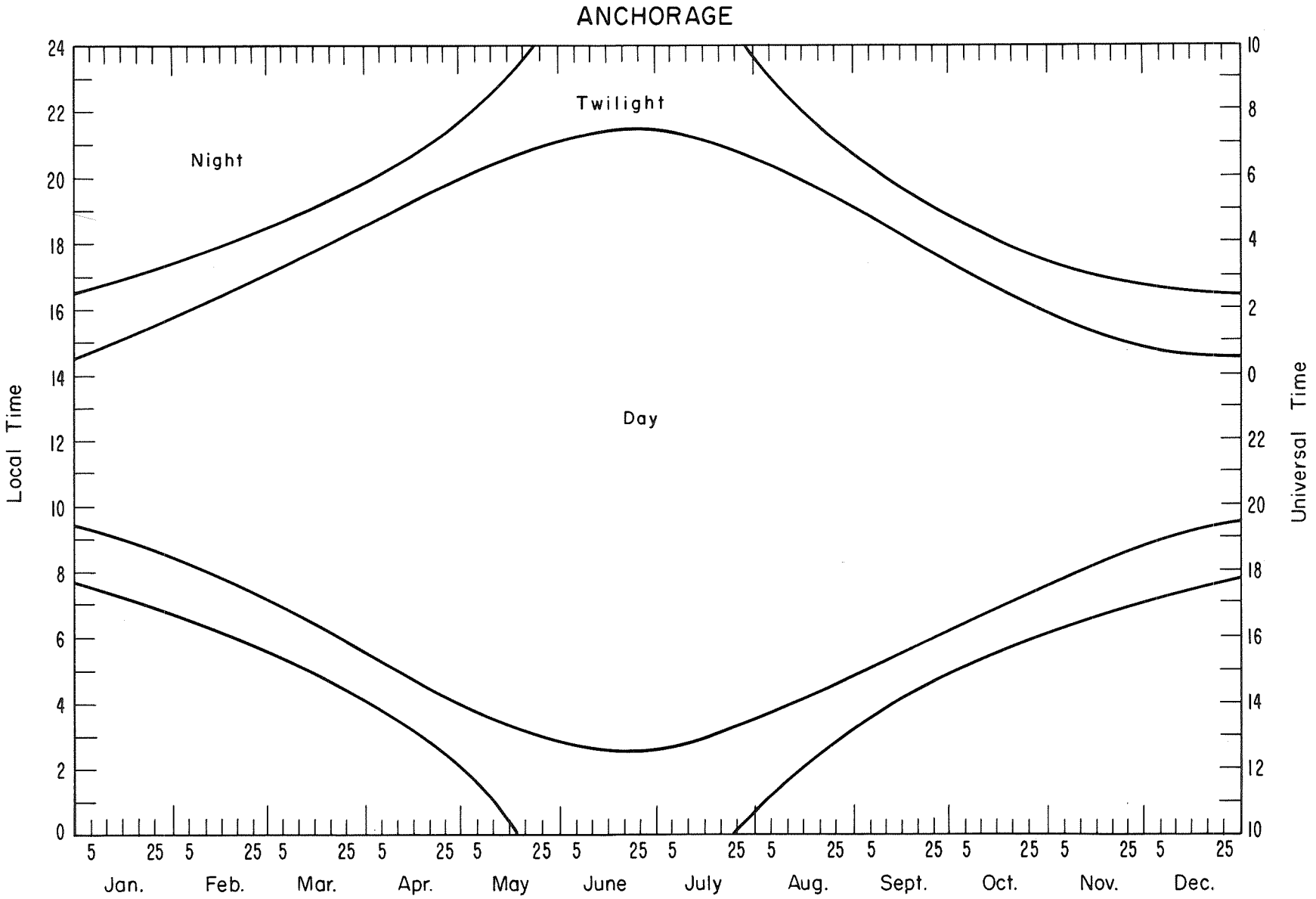

Figure 4. Solar illumination plot - Anchorage.

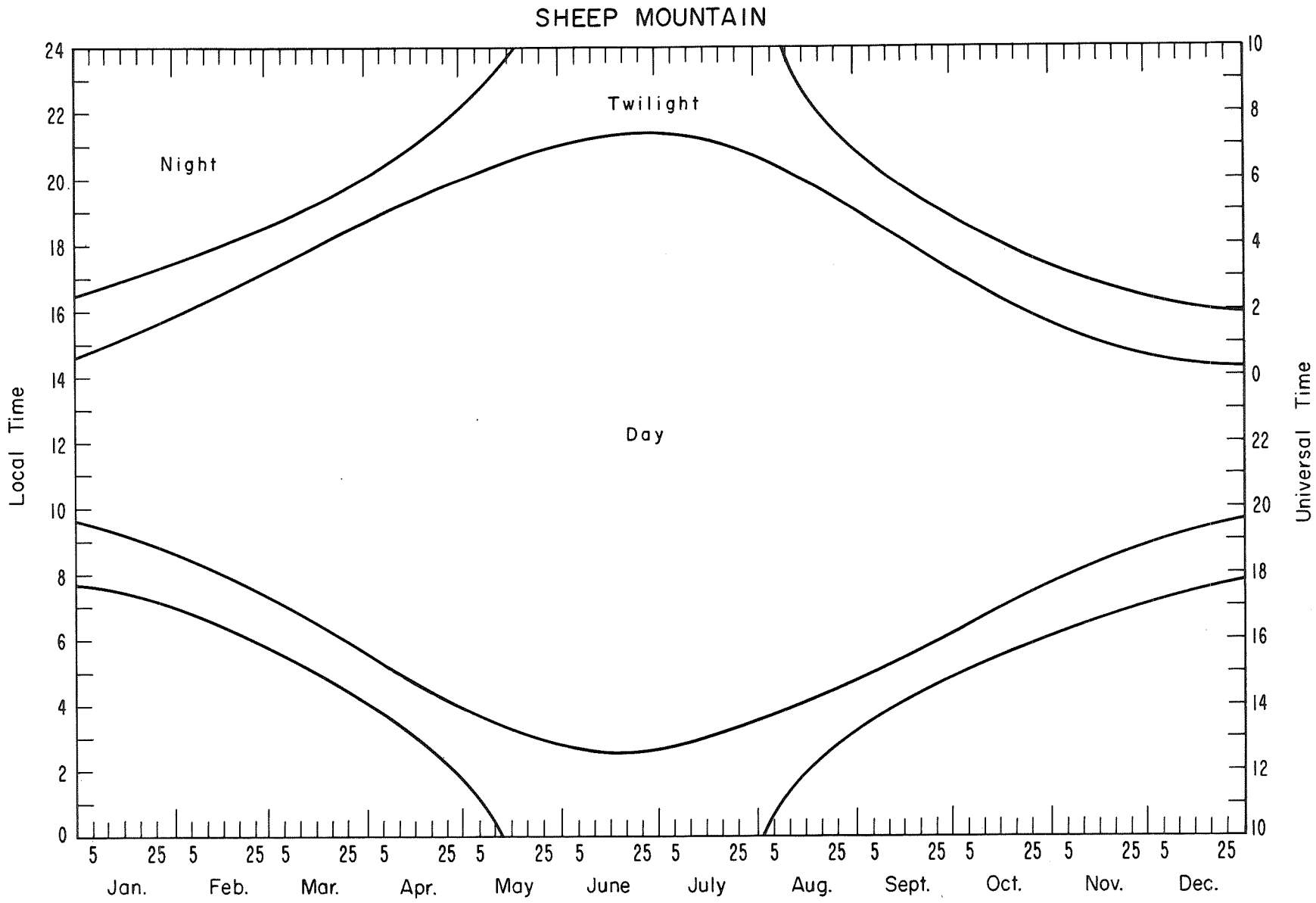

Figure 5. Solar illumination plot - Sheep Mountain.

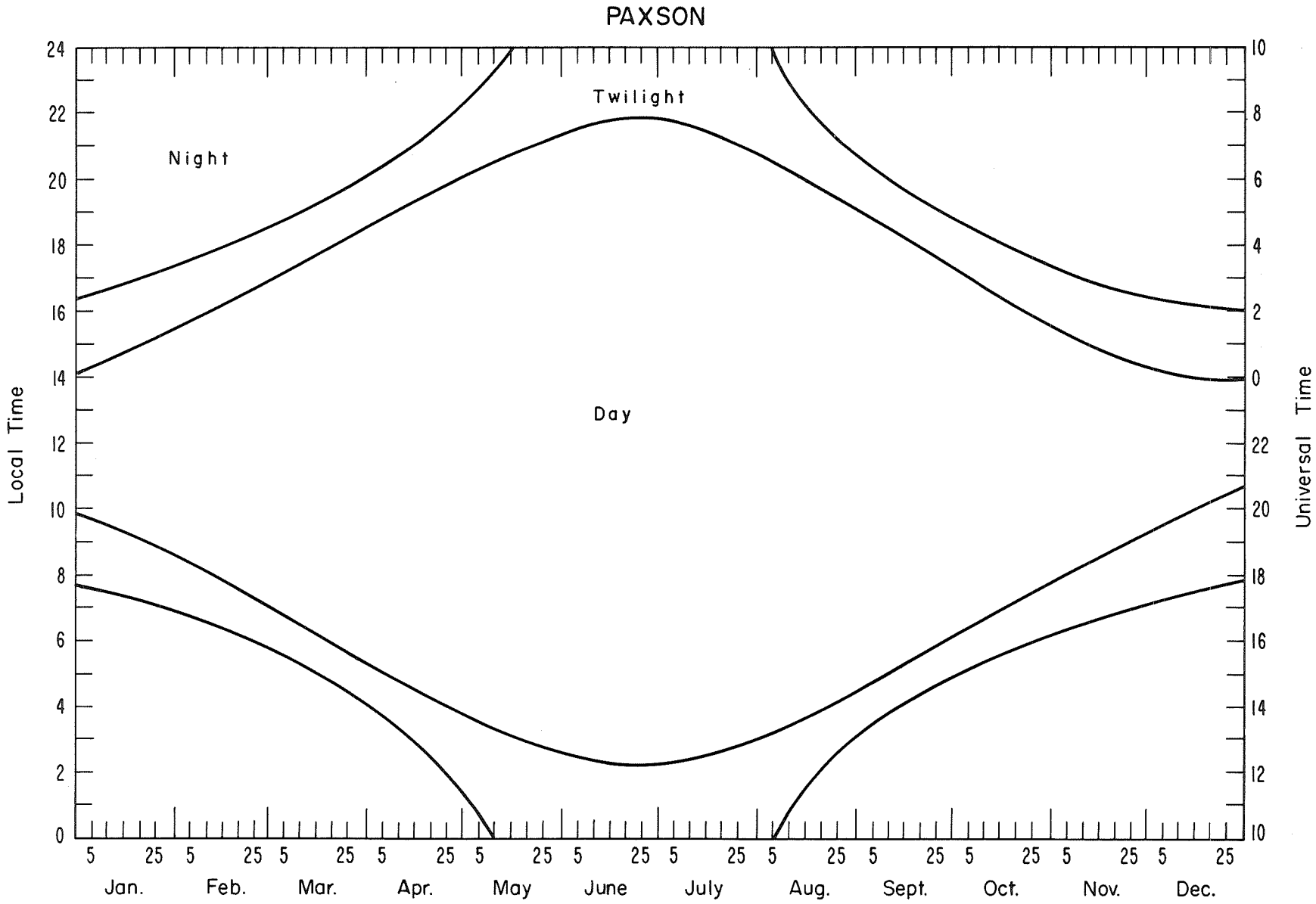

Figure 6. Solar illumination plot - Paxson.

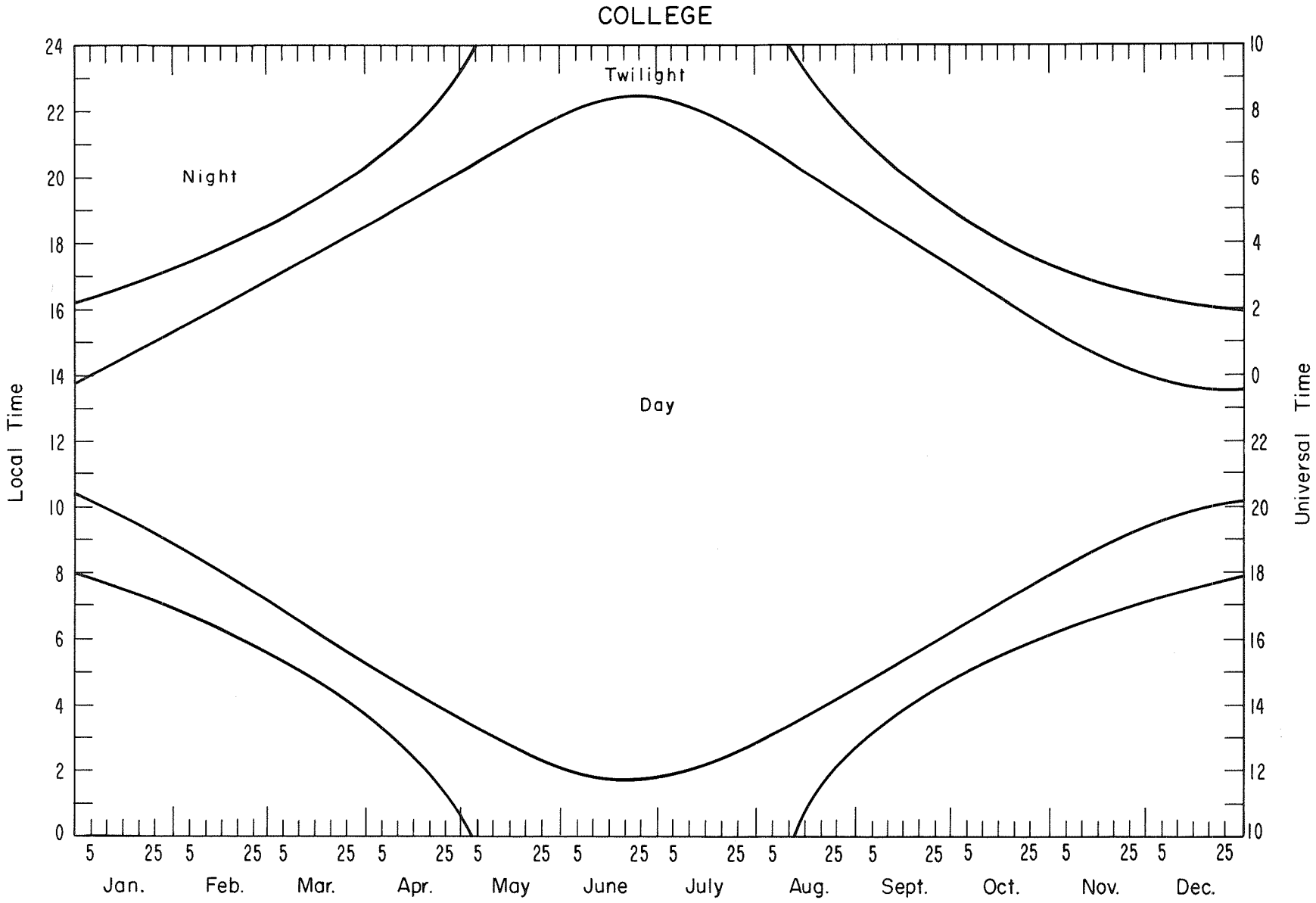

Figure 7. Solar illumination plot - College.

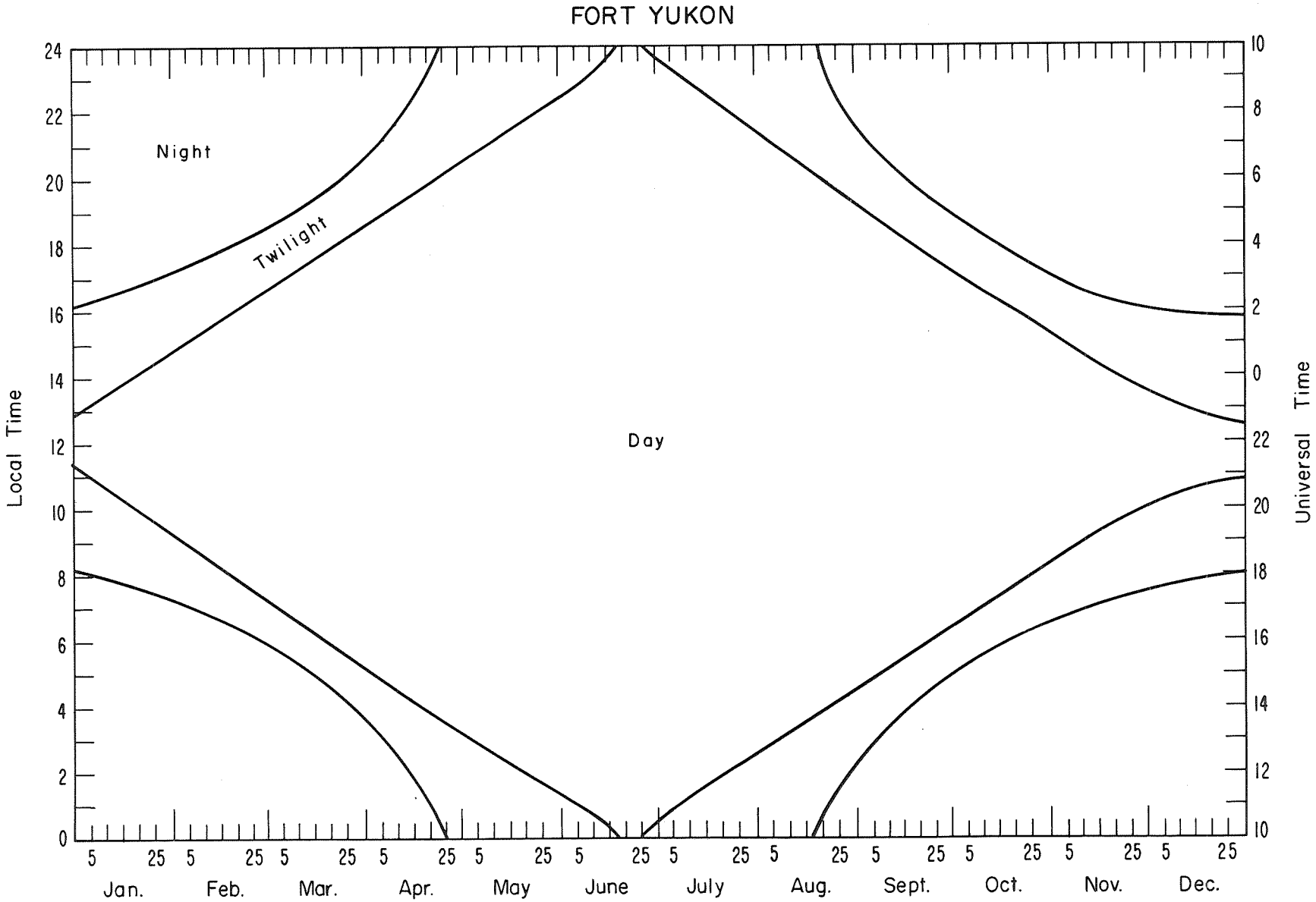

Figure 8. Solar illumination plot - Fort Yukon.

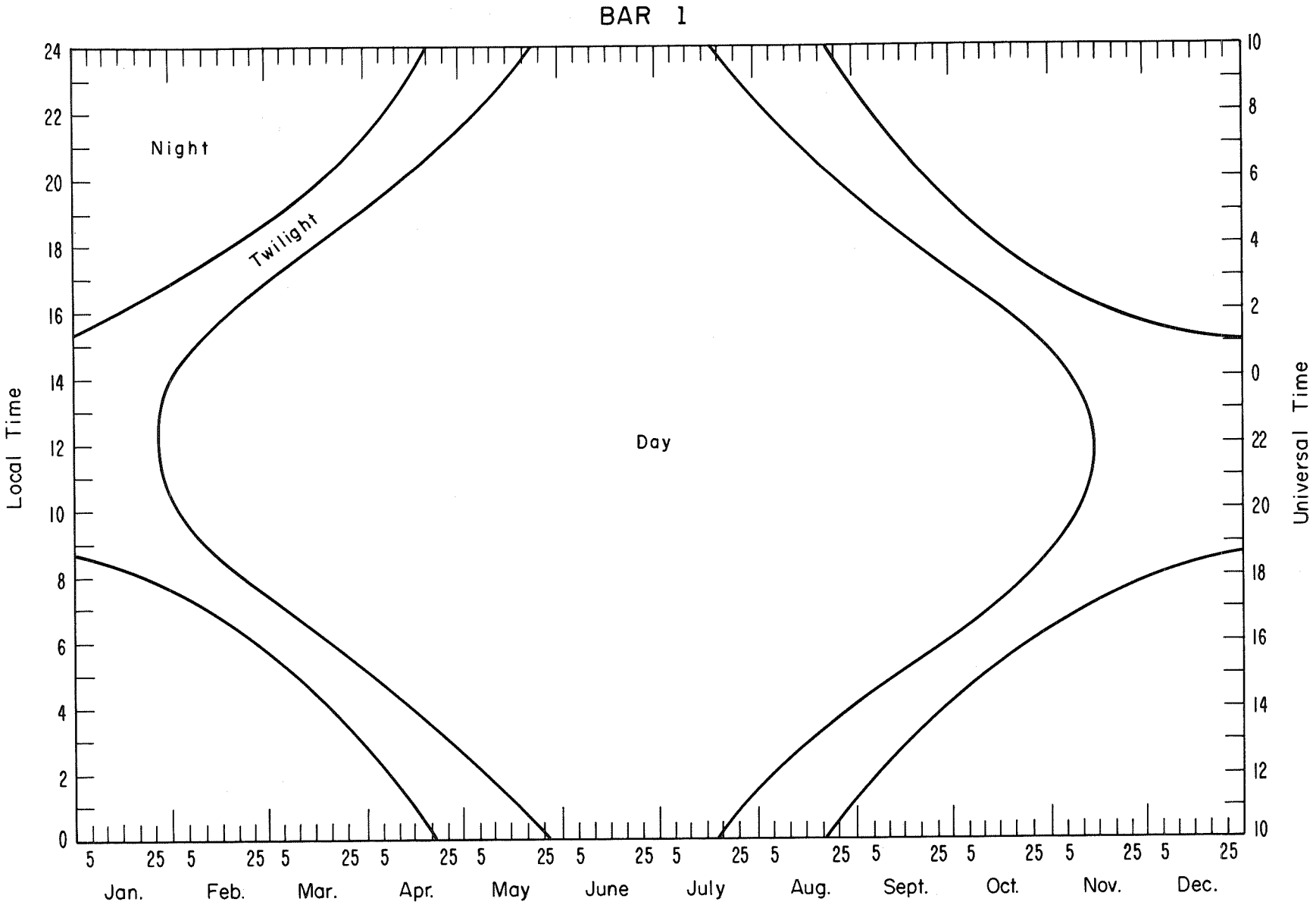

Figure 9. Solar illumination plot - Bar I

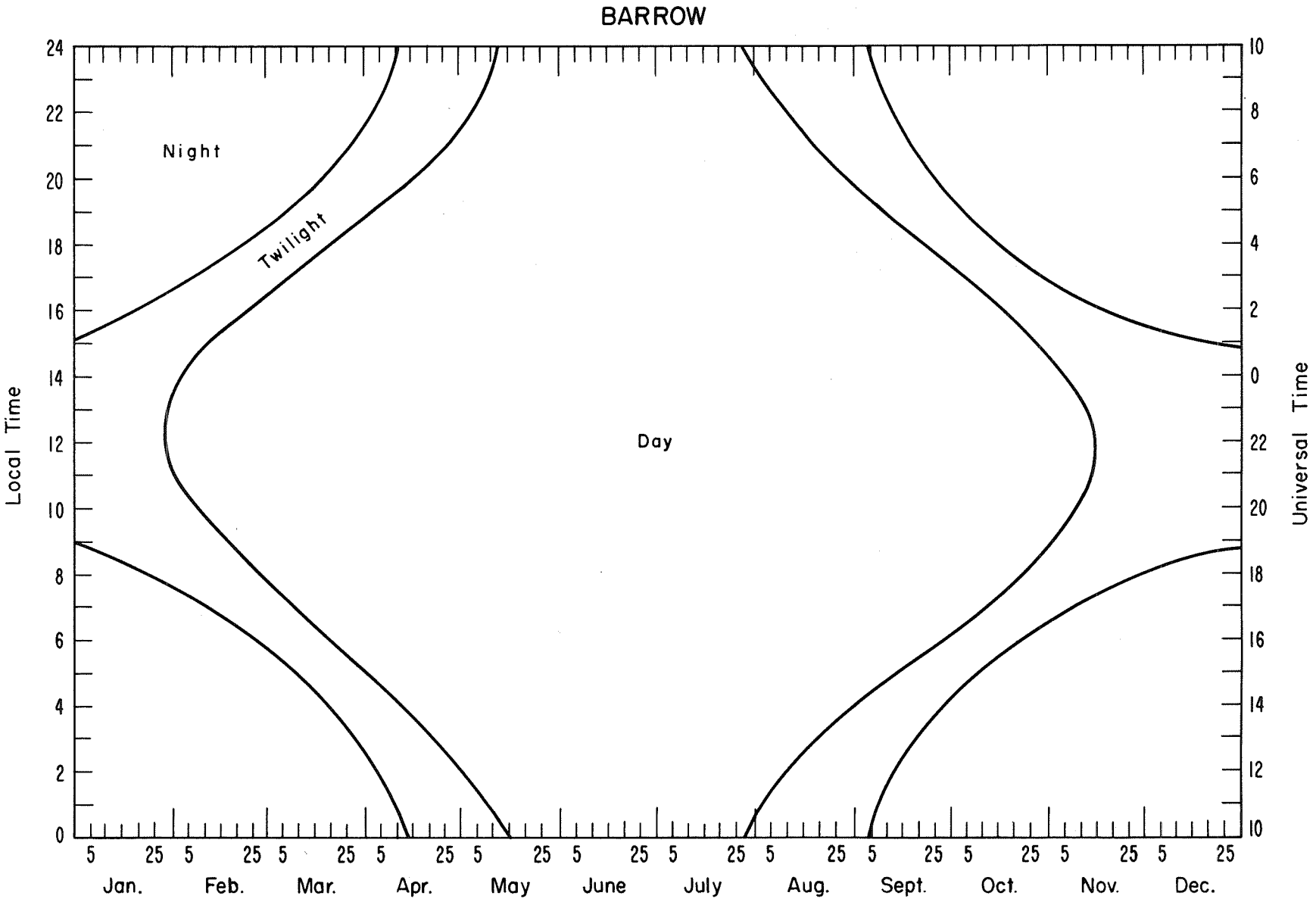

Figure 10. Solar illumination plot - Barrow.

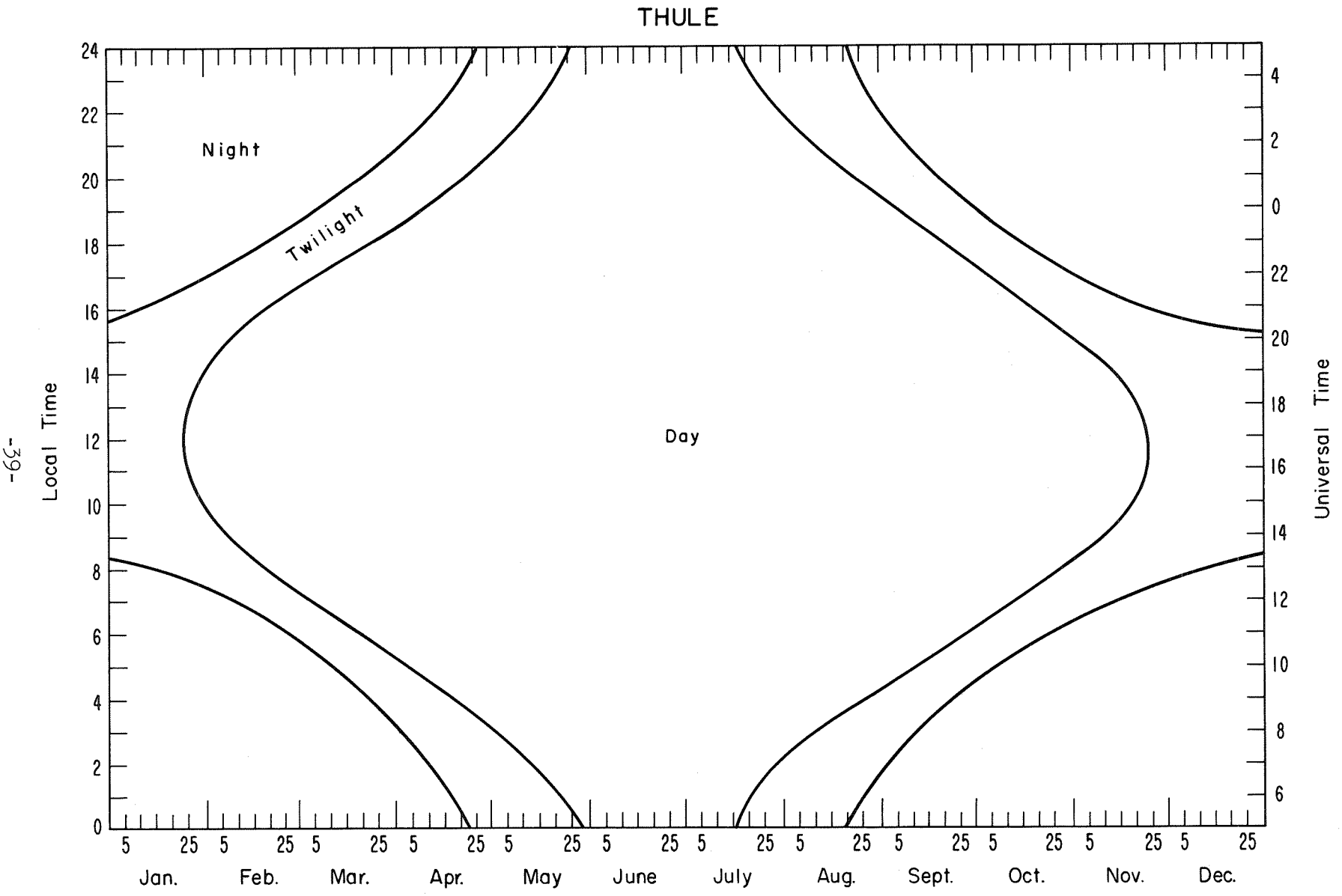

Figure 11. Solar illumination plot - Thule.

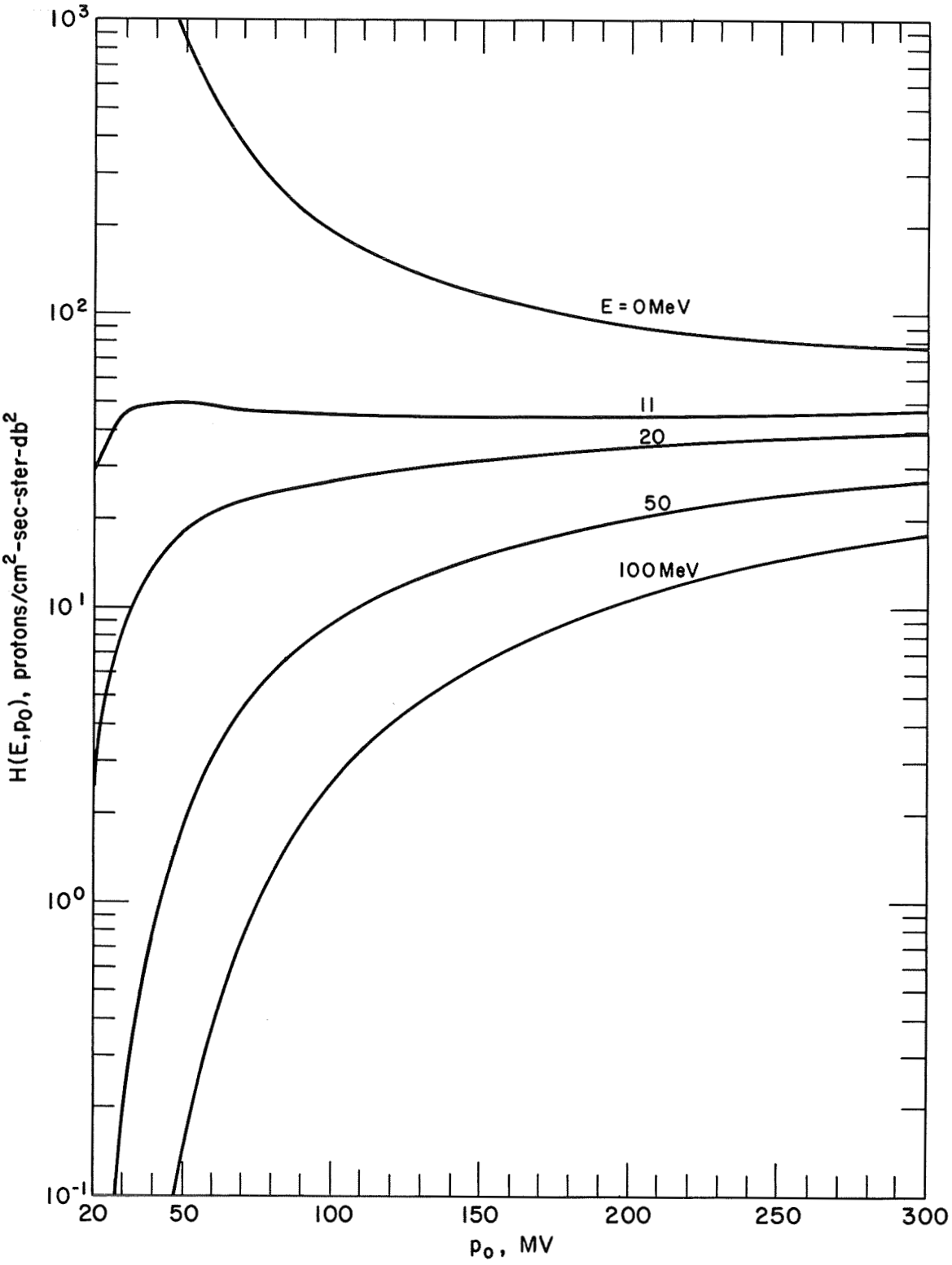

Figure 12. $H(E, p_o)$, defined as $J(>E)/A^2$, for a daytime, polar-cap, 30 MHz riometer. Note the constancy of the 11 MeV curve. 11 MeV is therefore E_{LS}, the least sensitive energy.

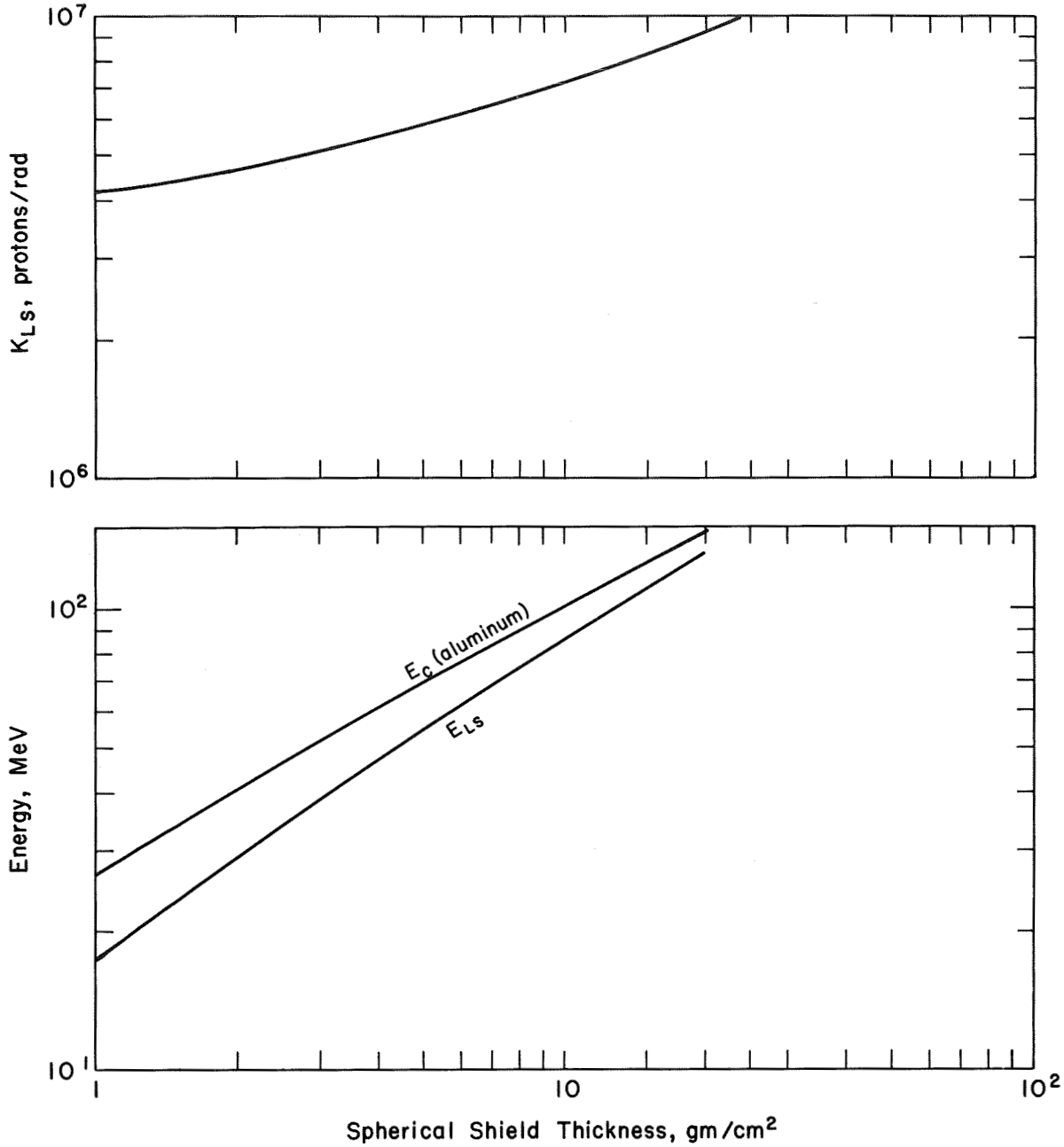

Figure 13. Top curve - K_{LS} (defined as J(>E)/D evaluated at E_{LS}, the least sensitive energy) as a function of shield thickness for a spherical aluminum shield. Bottom curves - the cutoff energy, E_c, and the least sensitive energy, E_{LS}, for a spherical aluminum shield.

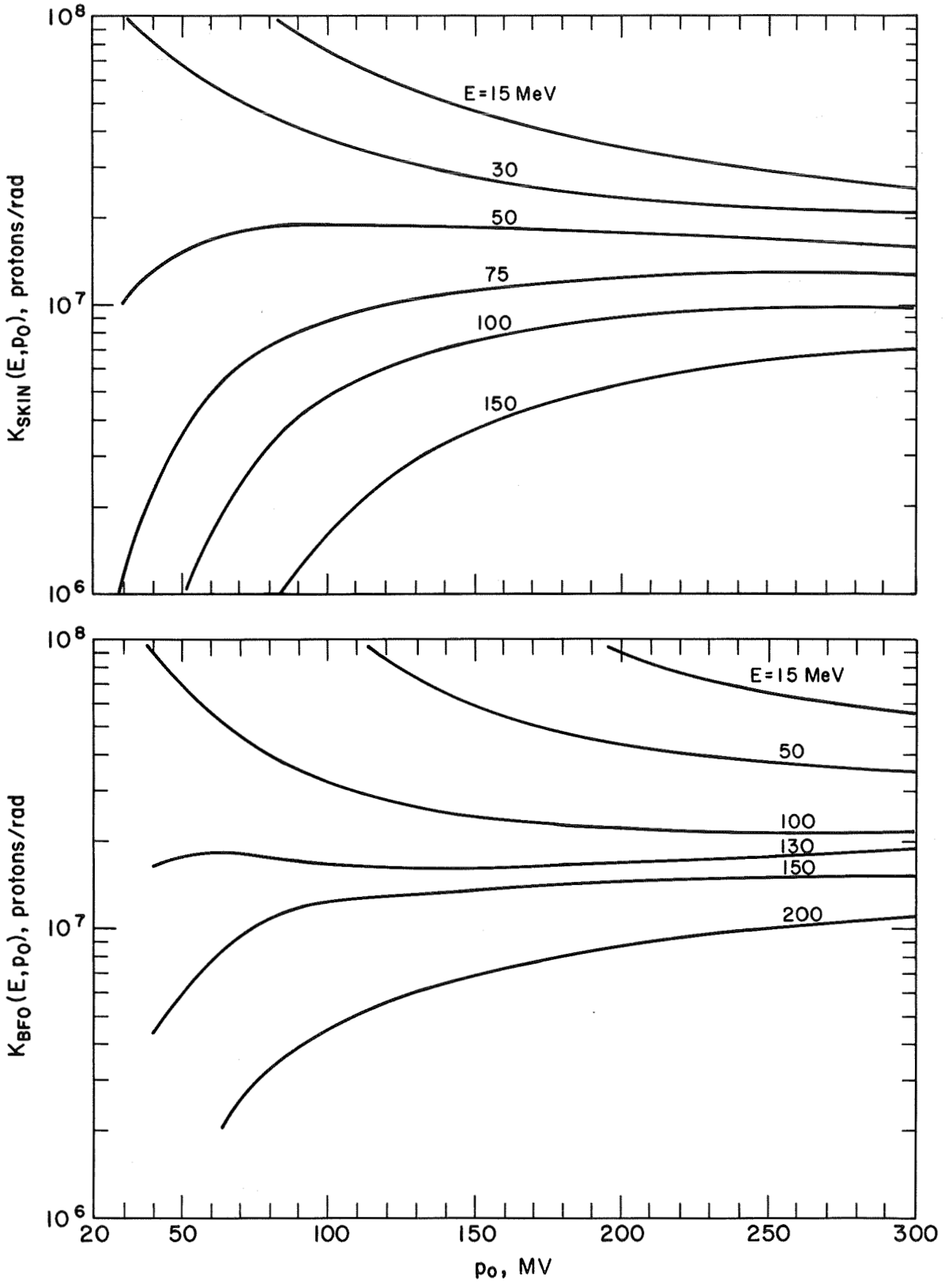

Figure 14. $K(E, p_o)$ for skin and BFO doses for the particular shielding geometry of the Apollo Command Module. The least sensitive energies are therefore 50 and 130 MeV.

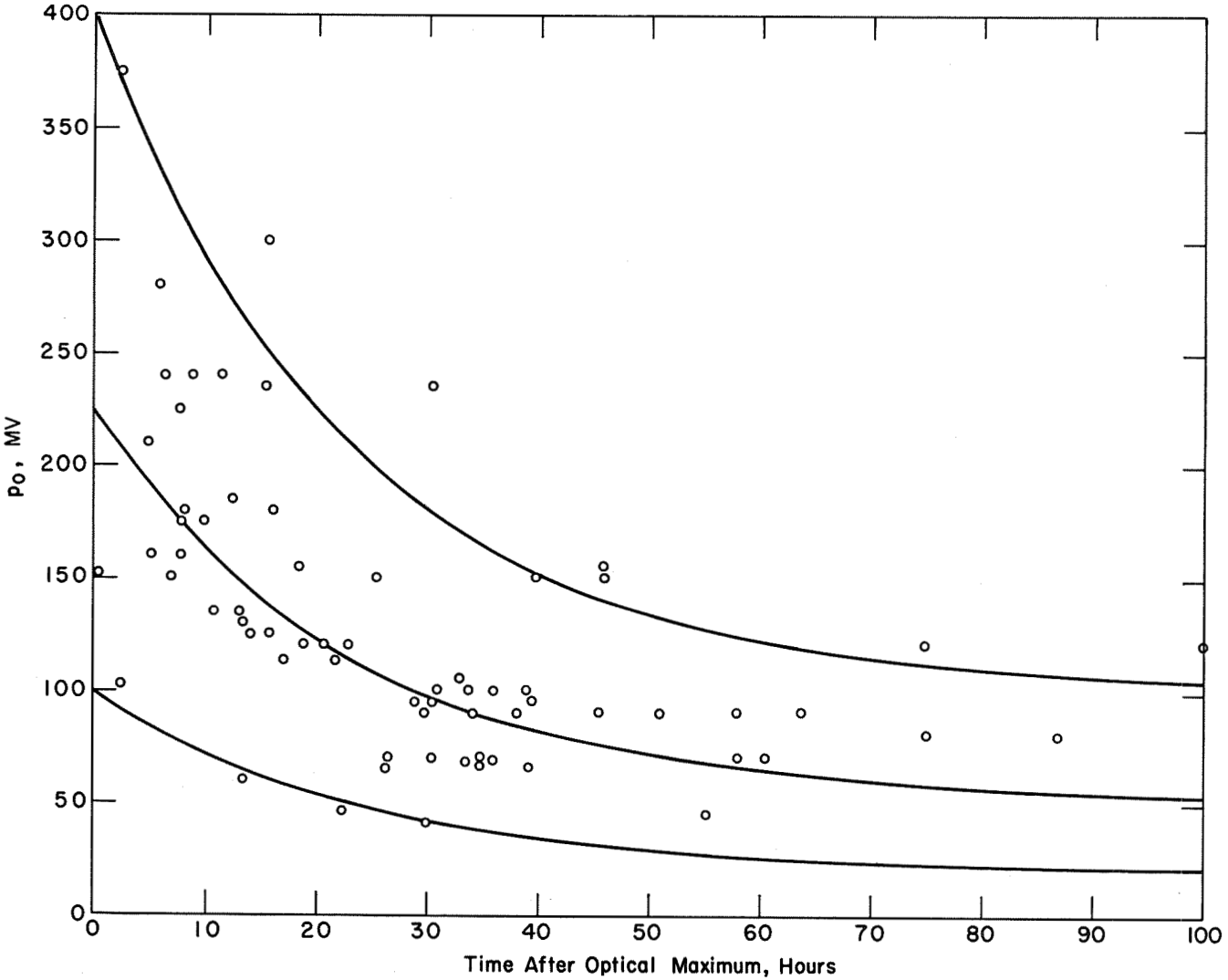

Figure 15. Individual points - p_o versus time from past solar cosmic ray events. Data taken from Freier and Webber (1963, table 2). Curves - hard, typical, and soft spectrum fits to the data.

GPO 852-464